Design of Single-Polarization Single-Mode Photonic Crystal Fiber at 1.30 and 1.55 μm

Jian Ju, Wei Jin, *Senior Member, IEEE*, and M. Suleyman Demokan, *Senior Member, IEEE*

***Abstract*—Single-polarization single-mode (SPSM) operation of a highly birefringent (HB) photonic crystal fiber (PCF) is investigated in detail by using a full-vector finite-element method (FEM) with anisotropic perfectly matched layers (PMLs). The cutoff wavelengths of the two linearly polarized principal states can be designed by varying the structure parameters of the PCF. The confinement loss and splice loss to standard single-mode fiber for particular SPSM PCFs are calculated and optimized at both 1.30 and 1.55 μm.**

***Index Terms*—Confinement loss, finite-element method, photonic crystal fiber, single-polarization single-mode fiber.**

I. Introduction

PHOTONIC crystal fibers (PCFs) have attracted significant attention recently [1]–[4]. A PCF consists of a central core of air or pure silica surrounded by an array of air holes running along its length. PCFs may be divided into two categories: the index guiding PCF, where light is guided by modified total internal reflection [2], [3], and the bandgap guiding PCF, where light guiding is based on the effect of photonic bandgap (PBG) within which light propagation is prohibited [4].

The large index contrast and the stack-and-draw fabrication process permit high birefringence to be easily realized on PCFs. PCFs have been made highly birefringent (HB) by having different air hole diameters along the two orthogonal axes [5]–[7] or by asymmetric core design [8]–[10]. These fibers have demonstrated modal birefringence of an order of magnitude higher than that of the conventional HB fibers. Recently, a nonlinear PCF with birefringence higher than 7×10^{-3} has been reported [11]. Conventional HB fibers can be made to operate in the single-polarization single-mode (SPSM) regime in which only one linearly polarized mode is guided while the mode with orthogonal polarization is suppressed [12]–[14]. Recently, it has been shown that HB PCFs have the potential to realize better SPSM fibers [15], [16]. In [15], a low-loss SPSM PCF with a confinement loss of less than 0.1 dB/km from 1.48 to 1.6 μm was proposed and analyzed. Kubota *et al.* reported a PCF-based absolutely single polarization fiber (ASPF) with a polarization-dependent loss of 196 dB/km with a transmission loss of 28 dB/km at 1550 nm [16].

Although some preliminary conclusions have been drawn in [16], the reported PCF is not optimized for particular applications such as fiber polarizing devices. For example, to make a fiber polarizer with an extinction ratio of 30 dB at 1550 nm, it requires $\sim$ 150 m of such a fiber. Also, no explicit design criteria have been proposed for the design of SPSM PCF. It was therefore felt that more extensive design details were desirable. In this paper, we numerically explored the single-polarization operation for an HB PCF with a similar structure. The effects of varying PCF parameters on the characteristics of SPSM operation are discussed and general design criteria are given in Section II. A full-vector finite-element method (FEM) with perfectly matched layers (PMLs) as absorbing boundary conditions is used to analyze the polarization-dependent loss in Section III. Section IV describes the coupling efficiency between SPSM PCF and conventional singe-mode fiber (SMF) and recommends proper fiber parameters for 1.30- and 1.55-μm operation. A brief summary is given in Section V.

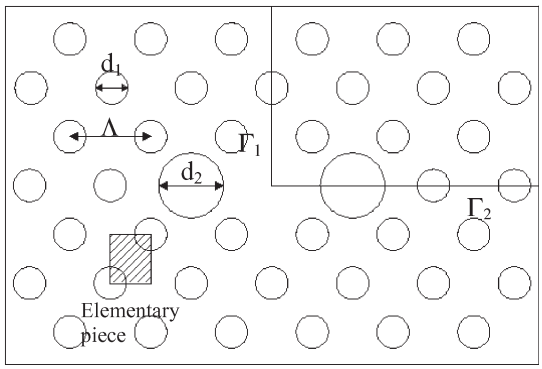

Fig. 1. Schematic cross-section of an HB PCF.

II. Design of SPSM PCF

The structure of the HB PCF to achieve single-polarization operation is assumed to be as shown in Fig. 1. It should be noticed that PCF with similar cross-sections can be HB because of different air hole diameters along the orthogonal axis [6], [7]. It is thus meaningful to find the proper PCF parameters that support only a single linearly polarized mode. To the author's knowledge, design details have not been reported. Although Kubota *et al.* have suggested that the condition for single polarization to be $d_2/d_1 > 2$ [16], we found that this is inadequate to assure single-polarization operation.

In this paper, a full-vector FEM [17], [18] is applied to analyze the dispersion properties of the HB PCF. Because of the symmetric nature of the PCF, only a quarter of the cross-section was used during the simulation and a perfect electric or perfect magnetic conductor (PEC or PMC) is applied along the symmetric plane Γ_1 and Γ_2. PEC or PMC makes the electric field perpendicular or parallel to the boundaries, respectively. The

Manuscript received October 8, 2004; revised October 12, 2005.

The authors are with the Department of Electrical Engineering, The Hong Kong Polytechnic University, Hung Hom, KLN, Hong Kong (e-mail: jianju.ee@polyu.edu.hk).

Digital Object Identifier 10.1109/JLT.2005.861942

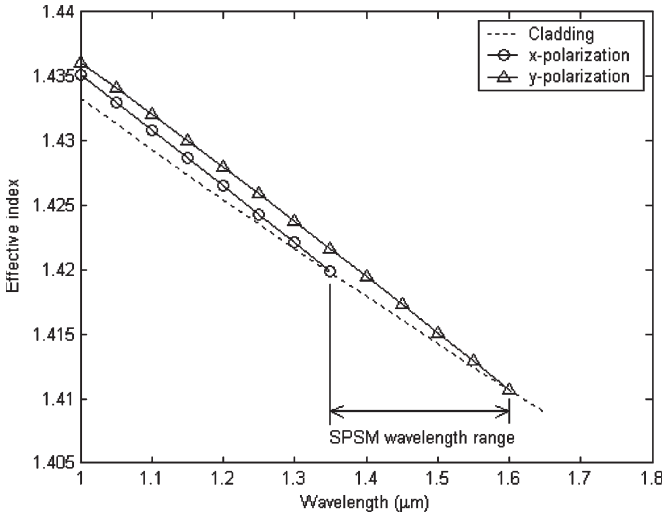

Fig. 2. Dispersion curves as a function of wavelength for PCF with $\Lambda = 2.2\ \mu$m, $d_1/\Lambda = 0.40$, and $d_2/\Lambda = 0.95$.

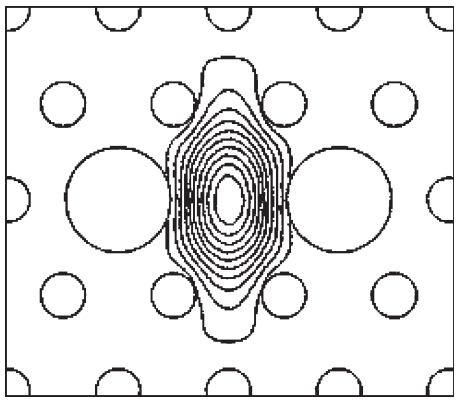

Fig. 3. Contour plot of intensity distribution of the PCF with $\Lambda = 2.2\ \mu$m, $d_1/\Lambda = 0.40$, and $d_2/\Lambda = 0.95$ at 1.55 μm.

polarization of a considered mode over a quarter of the cross-section is preserved subject to the proper choice of PEC and PMC combinations [18]. The computational window is chosen beforehand so that the influence of artificial outer boundaries can be neglected. The background refractive index was obtained from the Sellmeier equation for silica [19].

Fig. 2 shows the effective index of the x- and y-polarization mode as a function of wavelength for the PCF with $\Lambda = 2.2\ \mu$m, $d_1/\Lambda = 0.40$, and $d_2/\Lambda = 0.95$. Also shown in Fig. 2 is the effective index (cladding index) of the fundamental space-filling mode (SFM) [3], which is evaluated by applying FEM to the elementary piece as shown in Fig. 1. Polarization cutoff occurs when the effective index of one of the polarization states falls below that of the SFM. The cutoff wavelengths of x- and y-polarized modes are estimated to be ~ 1.37 and $\sim 1.62\ \mu$m, respectively, corresponding to the intersection points of their dispersion curves with that of the cladding dispersion as shown in Fig. 2. The single-polarization wavelength range where only the y-polarized mode is guided and the x-polarized mode is leaky is shown in the figure. Fig. 3 shows the intensity distribution of the y-polarized mode for the PCF at $1.55\ \mu$m. The mode is well confined and elongated in the y-direction.

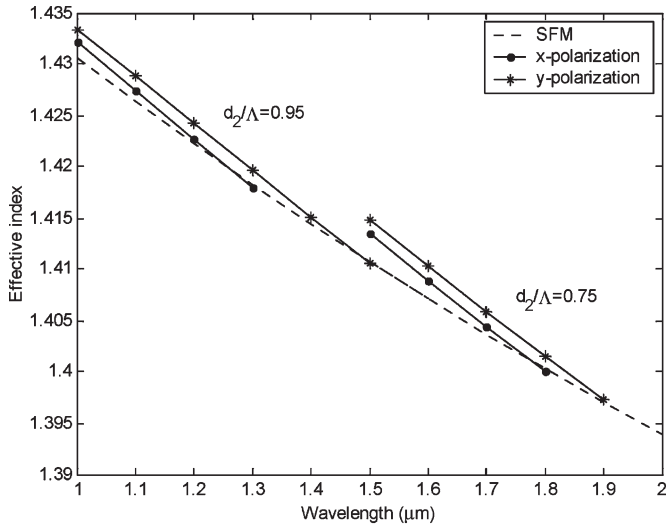

Fig. 4. Dispersion curves for SPSM PCF with different pitches d_2/Λ. The ratio d_1/Λ and pitch Λ are fixed at 0.40 and 2 μm, respectively.

We found that it is possible to tune the wavelength range for single-polarization operation by varying the fiber structural parameters: d_1/Λ, d_2/Λ, and Λ. Therefore, it is worthwhile to examine the dispersion properties under the influence of these parameters. First, we fixed d_1/Λ at 0.4 and Λ at 2 μm and changed d_2/Λ from 0.95 to 0.75 (Fig. 4). The cutoff wavelength for x- and y-polarization shifts from 1.26 and 1.48 μm to 1.78 and 1.915 μm, respectively. Tuning the cutoff wavelength by changing the d_2/Λ ratio is possible but at the cost of the reduction of single-polarization wavelength range from 220 to 135 nm for $d_2/\Lambda = 0.95$ to 0.75. The single-polarization wavelength length reduction can be attributed to the reduced birefringence induced by decreasing the diameter of the two big air holes. When the dispersion curves of x- and y-polarization are intercepted by that of the cladding mode, a smaller single-polarization wavelength range appears for $d_2/\Lambda = 0.75$. Therefore, d_2/Λ should be set as high as possible to attain a wider single-polarization wavelength range. $d_2/\Lambda = 0.95$ is a reasonable parameter for practical PCFs [20], and we assume this value for all the following simulations.

The hole pitch Λ is then varied from 1.6 to 2.4 μm in steps of 0.4 μm, where d_1/Λ and d_2/Λ are fixed at 0.40 and 0.95. The dispersion curves are shown in Fig. 5. The cutoff wavelength for x- and y-polarization shifts to longer wavelength with the increase of pitches, and the single-polarization wavelength range increases slightly. It is also possible to tune the cutoff wavelength by varying the ratio d_1/Λ. However, the pitch Λ should be varied accordingly in order for the fiber to be a single-polarization fiber over a useful wavelength range. Fig. 6 shows dispersion curves for two set of parameters of $d_1/\Lambda = 0.5$ and $\Lambda = 1.25\ \mu$m, and $d_1/\Lambda = 0.4$ and $\Lambda = 2\ \mu$m. A smaller ratio of d_1/Λ requires a larger pitch Λ to support a single polarization within a particular wavelength range. If the pitch Λ were kept constant, reduction of d_1/Λ to small values could lead to the dispersion curves of both polarizations becoming parallel to that of cladding, i.e., no crossing between the dispersion curves. Hence, the fiber would not be a single-polarization fiber any more. It is found that a PCF with a pitch as large as 8 μm

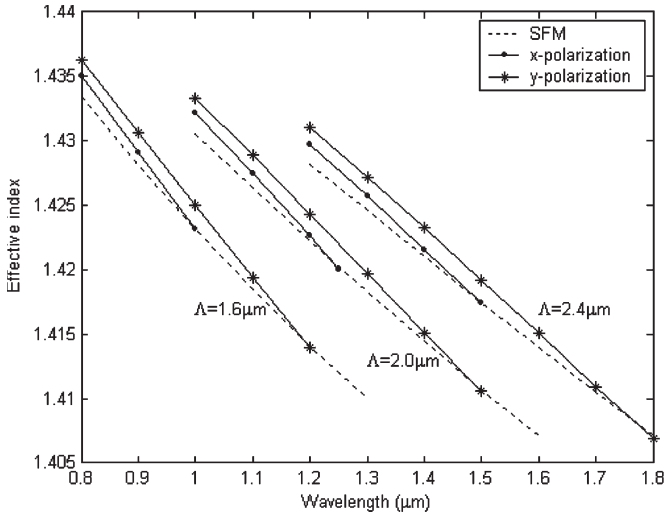

Fig. 5. Dispersion curves for SPSM PCF with different pitches Λ. The ratios d_1/Λ and d_2/Λ are fixed at 0.40 and 0.95, respectively.

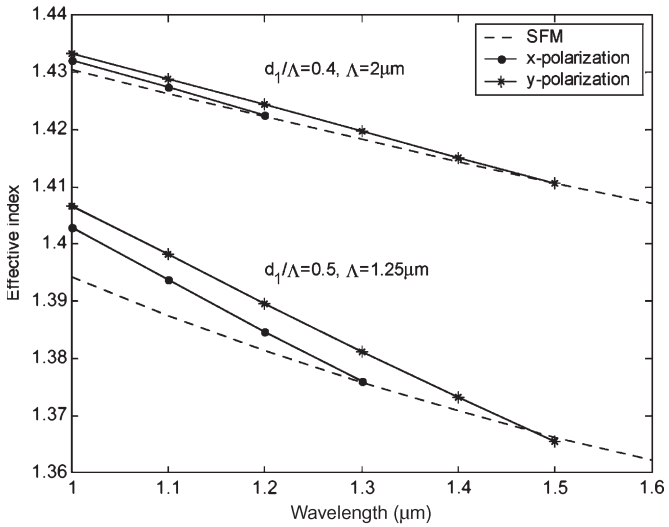

Fig. 6. Dispersion curves for SPSM PCF with different pitches d_1/Λ and pitches Λ. The ratio of d_2/Λ is fixed at 0.95.

and $d_1/\Lambda = 0.30$ has cutoff wavelengths of 1.12 and 1.8 μm for x- and y-polarization, respectively.

In order to find suitable parameters of d_1/Λ and Λ for SPSM operation, a series of numerical simulations have been performed. The cutoff wavelength as a function of Λ for different d_1/Λ is shown in Fig. 7. For smaller d_1 to Λ ratio, larger Λ values can be chosen to obtain a wider single-polarization range. The wide single-polarization wavelength range is easy to understand because the modal birefringence increases with a decrease of d_1/Λ, resulting in a wider intersection section between the dispersion curves of the guided modes and that of the cladding mode. As shown in Fig. 7(d), a d_1/Λ of 0.5, corresponding to d_2/d_1 of less than 2, indeed supports a single-polarization PCF although resulting in a narrow sing-polarization range.

From Fig. 7, we note that the cutoff wavelength shows linear dependence on Λ, which is useful for SPSM PCF design. The fiber structure parameters for a desirable SPSM PCF operating at a special wavelength can be easily obtained from Fig. 7.

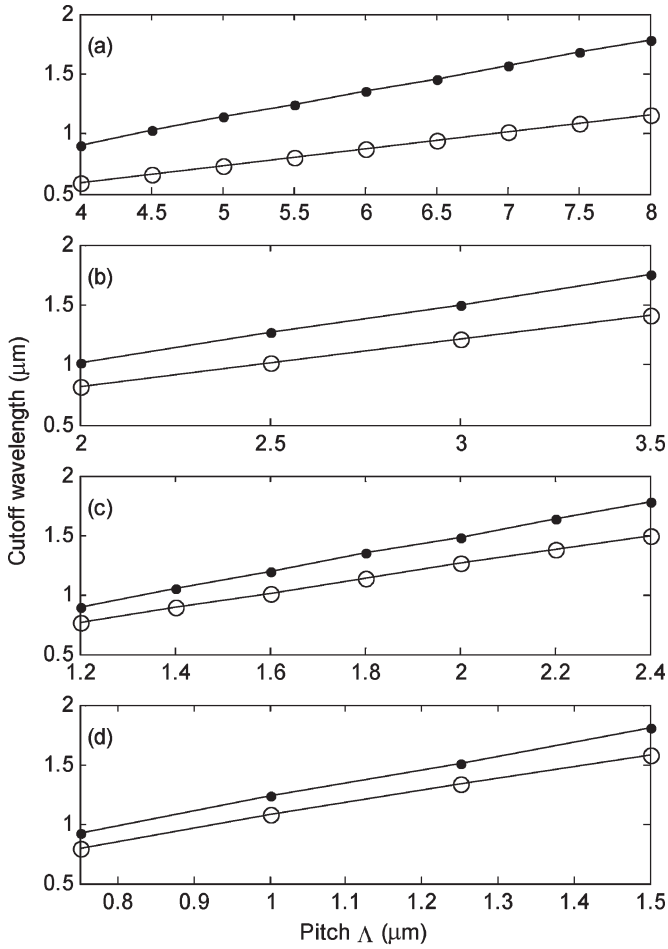

Fig. 7. Cutoff wavelength as a function of pitch Λ for different ratios of d_1/Λ. (a) $d_1/\Lambda = 0.3$, (b) $d_1/\Lambda = 0.35$, (c) $d_1/\Lambda = 0.4$, and (d) $d_1/\Lambda = 0.5$.

III. Polarization-Dependent Confinement Loss and Effective Area

Because the cladding of PCF is usually made of finite numbers of rings of air holes, the guided modes in PCF are inherently leaky. Various numerical methods have been applied to investigate the leakage properties of PCF [21], [22]. In this section, a full-vector FEM with anisotropic PMLs is used to find polarization-dependent confinement loss. We will show that confinement loss simulation can provide valuable information for designing SPSM PCFs. It should be mentioned that there are other loss mechanisms such as material absorption, Rayleigh scattering, and waveguide imperfections. The losses due to these factors are, compared with confinement loss, in general small and relatively independent of polarization, and hence are neglected here.

First, our FEM program was tested by rigorously comparing with the multipole method [21] and other FEM data [15], [22] before it is used to perform confinement loss calculation. Fig. 8 shows the calculated confinement loss of a nonbirefringent PCF (i.e., $d_1 = d_2 = d$) as a function of the number of rings of the hexagonally arranged air holes and d/Λ ratio, where d is the diameter of air hole and Λ is the hole spacing that is fixed at 2.3 μm [21]. These results are calculated using our FEM program and agree well with the published results, and therefore

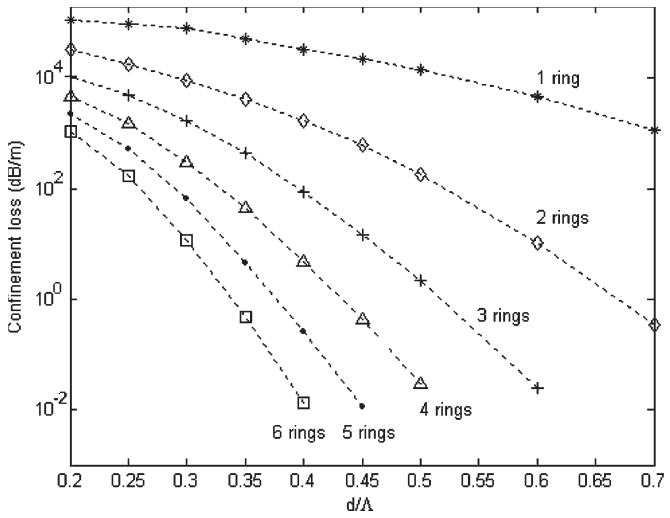

Fig. 8. Confinement loss as a function on the number of hexagonally arranged air holes and d/Λ for a wavelength of 155 μm. The air hole pitch is assumed to be 2.3 μm [21].

TABLE I
SPSM PCF PARAMETERS AND CONFINEMENT LOSS AT 1300 nm

	PCF I	PCF II	PCF III	PCF IV
d_1/Λ	0.30	0.35	0.40	0.50
Λ (μm)	9.03	3.22	2.07	1.21
Confinement Loss (dB/m)	*x*: 4.55 *y*: 0.11	*x*: 40.61 *y*: 0.33	*x*: 108.3 *y*: 0.56	*x*: 1692.1 *y*: 7.85
Bandwidth (nm)	14.6	84.7	65.3	41.7

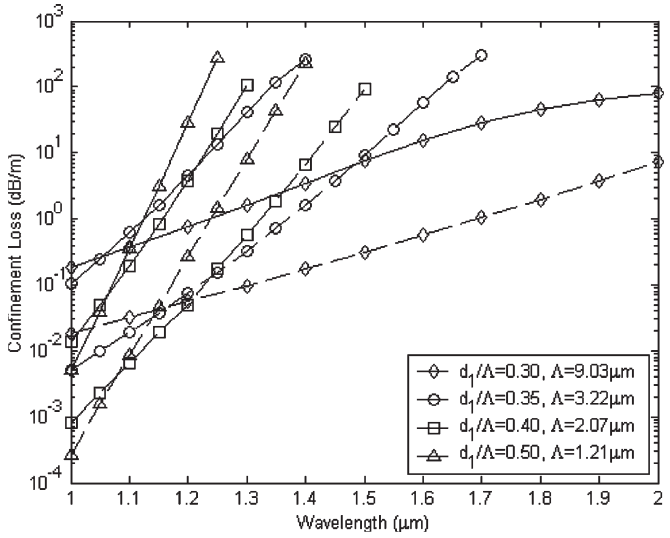

Fig. 9. Confinement loss for the x- and y-polarization for SPSM PCF working at 1.30 μm. Solid lines: x-polarization; dashed lines: y-polarization.

we conclude that our program is reliable for confinement loss calculation.

We first study the PCFs aiming for single-polarization operation around 1.30 μm. The PCF parameters with cutoff wavelength of 1.30 μm are listed in Table I. These parameters were obtained by setting the cutoff wavelength of the x-polarization to 1.30 μm and calculating the corresponding pitches for various d_1/Λ ratios. Fig. 9 shows the confinement losses for x- and

TABLE II
SPSM PCF PARAMETERS AND CONFINEMENT LOSS AT 1550 nm

	PCF V	PCF VI	PCF VII	PCF VIII
d_1/Λ	0.30	0.35	0.40	0.50
Λ (μm)	10.797	3.854	2.479	1.457
Confinement Loss (dB/m)	*x*: 1.5427 *y*: 0.0832	*x*: 32.286 *y*: 0.2665	*x*: 87.897 *y*: 0.4758	*x*: >1000 *y*: 5.1234
Bandwidth (nm)	12.4	103.5	72.9	45.6

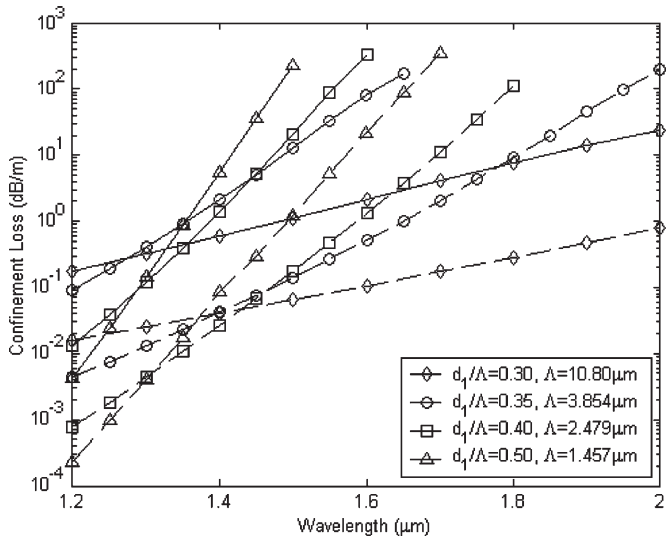

Fig. 10. Confinement loss for the x- and y-polarization for SPSM PCF working at 1.55 μm. Solid lines: x-polarization; dashed lines: y-polarization.

y-polarization with eight rings of air holes. The confinement losses for x- and y-polarized modes and SPSM bandwidth (BW) are also given in Table I. The SPSM BW is defined as the wavelength range over which one polarization state is attenuated by at least 30 dB/m while the orthogonal state suffers less than 1 dB/m. PCF II shows the largest BW and PCF I is the smallest, which can be easily understood from Fig. 9. In Fig. 9, we see that low confinement losses can be obtained for both polarization modes at wavelengths far from the cutoff values (e.g., 1.0 μm), whereas the confinement losses of x-polarization show an order of magnitude higher than that of y-polarization. PCF IV shows a sharp increase whereas PCF I reveals a gradual increase in confinement loss. The gradual increase can be attributed to the longer transition region between the cladding mode and the guided y-polarized mode. Compared with other SPSM PCFs listed, PCF I allows the largest hole spacing Λ, resulting in a small splice loss with conventional optical fiber. However, the confinement loss difference between x- and y-polarization is the smallest for PCF I, and the SPSM BW is only 14.6 nm compared to 84.7 nm of PCF II.

A similar confinement loss profile can be found at 1.55 μm (Table II and Fig. 10). Comparing the data provided in Tables I and II, a small increase in single-polarization bandwidth can be found, which confirms the data plotted in Fig. 7.

It has been shown that the mode field diameter (MFD) of a single-polarization optical fiber is a useful indicator of the fiber's performance [13], and the mode cutoff of PCF can also be studied from the corresponding effective area A_{eff} [23].

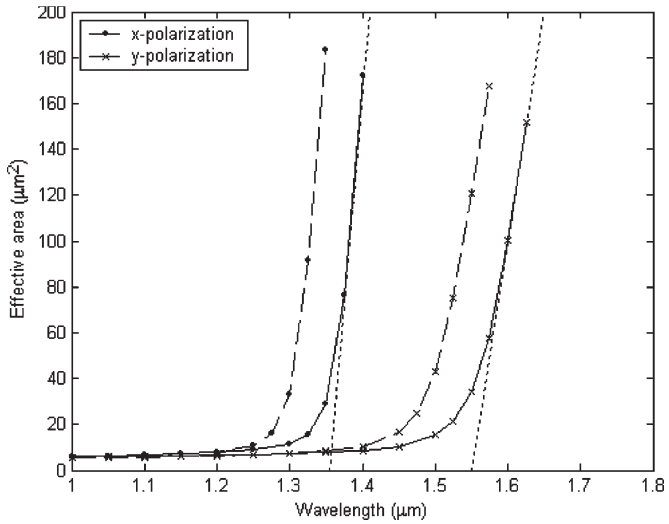

Fig. 11. Calculated effective area of the two polarization states of an SPSM PCF with $d_1/\Lambda = 0.40$, $\Lambda = 2.07$ μm (solid lines) and a modified PCF with $d_1/\Lambda = 0.40$, $\Lambda = 1.98$ μm (dashed lines). The crossing of the dotted lines with the horizontal axis indicates the cutoff wavelength for the x- and y- polarized states.

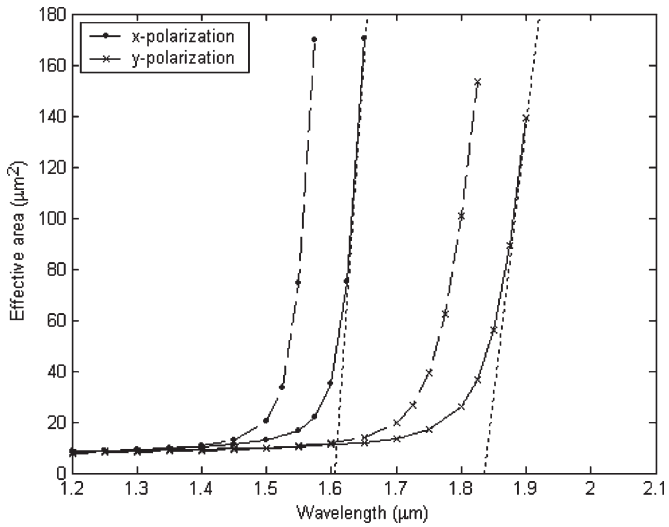

Fig. 12. Calculated effective area of the two polarization states of an SPSM PCF with $d_1/\Lambda = 0.40$, $\Lambda = 2.479$ μm (solid lines) and a modified PCF with $d_1/\Lambda = 0.40$, $\Lambda = 2.35$ μm (dashed lines).

The calculated A_{eff} of the SPSM PCF with $d_1/\Lambda = 0.40$, $\Lambda = 2.07$ μm (PCF III), as a function of wavelength is plotted in solid lines in Fig. 11. As has been shown in Fig. 7(c), this fiber has a cutoff wavelength of ~ 1.3 and ~ 1.5 μm for the x- and y-polarization states, respectively. It can be seen from Fig. 11 that A_{eff} remains nearly constant below the cutoff wavelength but increases dramatically above the cutoff. The cutoff wavelength may be defined here by the crossing of the dotted lines as shown in Fig. 11 with the horizontal axis [23], which are ~ 1.35 and ~ 1.55 μm, respectively, for the x- and y-polarized states. The discrepancy between the cutoff wavelengths obtained this way and that from Fig. 7 is less than 4%. From the practical point of view, the pitch Λ should be chosen to be a smaller value so that the cutoff wavelength shifts to a shorter wavelength. For comparison, we also showed the A_{eff} of a modified SPSM PCF with $d_1/\Lambda = 0.40$, $\Lambda = 1.98$ μm, in dashed lines in Fig. 11. The A_{eff} of the SPSM PCFs operating at 1.55 μm is shown in Fig. 12, where the solid lines and the dashed lines depict, respectively, the PCF with $d_1/\Lambda = 0.40$, $\Lambda = 2.479$ μm (PCF VII), and a modified PCF with $d_1/\Lambda = 0.40$, $\Lambda = 2.35$ μm.

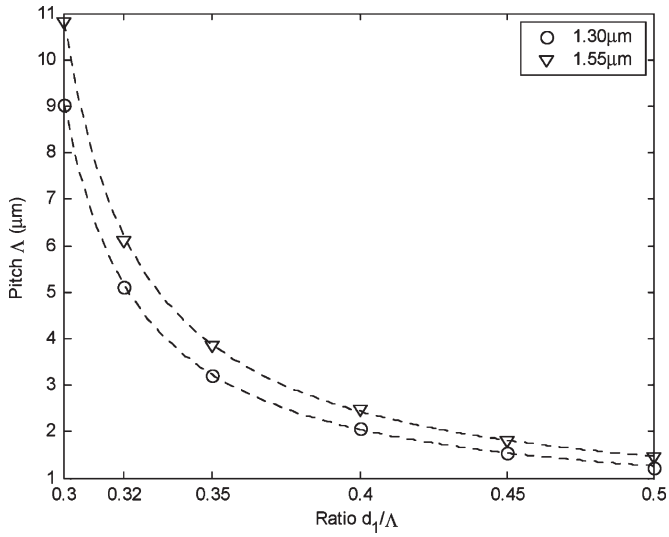

Fig. 13. Pitch Λ as a function of the ratio d_1/Λ for SPSM PCF with x-polarization cutoff wavelength of 1.3 and 1.55 μm. The dotted lines are curve fitting results.

IV. Coupling Efficiency

For practical applications of SPSM PCF, splice loss between single-polarization fiber and conventional fiber or other optical waveguide should be considered. The splice loss depends on a number of factors such as longitudinal, lateral, or angular misalignment. These factors are not considered here, and we only consider the ideal case where the two fibers are perfectly aligned. Under such conditions, the splice or joint loss may be estimated by using the well-known overlap integral method. We use a full-vector FEM to calculate the electrical field distributions of SPSM, which are then used to calculate the splice loss by evaluating the overlap integral of the fields of the SPSM and the single mode fiber.

Before the splice loss calculation, the relation of pitch Λ as a function of the ratio d_1/Λ for SPSM PCF with x-polarization cutoff wavelength of 1.30 and 1.55 μm is plotted in Fig. 13. The pitch associated with a specific ratio of d_1/Λ can be obtained from the curve fitting results (shown in dotted lines in Fig. 13). The coupling efficiency between SPSM PCFs and single-mode fiber (SMF) is calculated and shown in Fig. 14. In the simulations, the MFD of SMF is approximated by normalized Gaussian modes, and they are assumed to be 9.2 μm at 1.30 μm and 10.4 μm at 1.55 μm [24]. The mode field distribution of PCF is obtained by FEM and normalized before calculation. Overlap integration is then performed numerically to evaluate the coupling efficiency. Fig. 14 shows the coupling efficiency as a function of d_1/Λ. The maximal coupling efficiency is estimated to be $\sim 78\%$ and $\sim 77\%$ for 1.55 and 1.30 μm, respectively, and the corresponding PCF structures are $d_1/\Lambda = 0.32$, $\Lambda = 5.1754$ μm for 1.30 μm, and

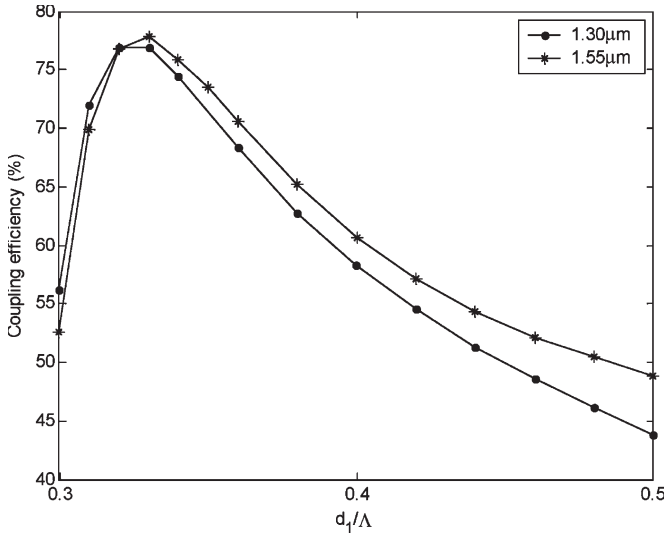

Fig. 14. Coupling efficiency as a function of d_1/Λ for 30 and 1.55 μm.

$d_1/\Lambda = 0.33$, $\Lambda = 5.1646$ μm for 1.55 μm. The polarization-dependent confinement loss is 6.51 dB/m for x-polarization and 0.179 dB/m for y-polarization at 1.30 μm and 6.78 dB/m (x-polarization) and 0.144 dB/m (y-polarization) at 1.55 μm. Apparently, these loss data are not within the single-polarization range as defined in Section III, indicating that optimal coupling and optimal polarization extinction ratio may not be achieved simultaneously. We recommend the use of $d_1/\Lambda = 0.35$ (PCF II and VI as shown in Tables I and II) for SPSM PCF as being the optimum. The coupling efficiency would be over 70% for both 1.30 and 1.55 μm.

V. Conclusion

In conclusion, we have described the design methodology of PCF for SPSM operation at a particular operating wavelength. The polarization-dependent confinement loss of SPSM PCF and coupling efficiency between SMF and PCF are numerically calculated as functions of PCF parameters and wavelengths. We show that the SPSM PCF can be optimized for 1.30- and 1.55-μm wavelength by choosing proper PCF design parameters. The BWs of the SPSM PCFs designed for 1.30- and 1.55-μm operation are, respectively, 84.7 and 103.5 nm within which one polarization state is attenuated by at least 30 dB/m while the orthogonal state suffers a loss of less than 1 dB/m. These PCFs may be found useful applications for all fiber polarizer.

References

[1] J. C. Knight and P. S. J. Russell, "Photonic crystal fibers: New way to guide light," *Science*, vol. 296, no. 5566, pp. 276–277, Apr. 2002.
[2] J. C. Knight, T. A. Birks, P. S. J. Russell, and D. M. Atkin, "All-silica single-mode optical fiber with photonic crystal cladding," *Opt. Lett.*, vol. 21, no. 19, pp. 1547–1549, Oct. 1996.
[3] T. A. Birks, J. C. Knight, and P. S. J. Russell, "Endlessly single-mode photonic crystal fiber," *Opt. Lett.*, vol. 22, no. 13, pp. 961–963, Jul. 1997.
[4] J. C. Knight, J. Broeng, T. A. Birks, and P. S. J. Russell, "Photonic band gap guidance in optical fibers," *Science*, vol. 282, no. 5393, pp. 1476–1478, Nov. 1998.
[5] A. Ortigosa-Blanch, J. C. Knight, W. J. Wadsworth, J. Arriaga, B. J. Mangan, T. A. Birks, and P. S. J. Russell, "Highly birefringent photonic crystal fibers," *Opt. Lett.*, vol. 25, no. 18, pp. 1325–1327, Sep. 2000.
[6] K. Suzuki, H. Kubota, S. Kawanishi, M. Tanaka, and M. Fujita, "High-speed bi-directional polarization division multiplexed optical transmission in ultra low-loss (1.3 dB/km) polarization-maintaining photonic crystal fiber," *Electron. Lett.*, vol. 37, no. 23, pp. 1399–1401, Nov. 2001.
[7] ——, "Optical properties of a low-loss polarization-maintaining photonic crystal fiber," *Opt. Express*, vol. 9, no. 13, pp. 676–680, Dec. 2001.
[8] T. P. Hansen, J. Broeng, S. E. B. Libori, E. Knuders, A. Bjarklev, J. R. Jensen, and H. Simonsen, "Highly birefringent index-guiding photonic crystal fibers," *IEEE Photon. Technol. Lett.*, vol. 13, no. 6, pp. 588–590, Jun. 2001.
[9] K. Saitoh and M. Koshiba, "Photonic bandgap fibers with high birefringence," *IEEE Photon. Technol. Lett.*, vol. 14, no. 9, pp. 1291–1293, Sep. 2002.
[10] P. R. Chaudhuri, V. Paulose, C. Zhao, and C. Lu, "Near-elliptic core polarization-maintaining photonic crystal fiber: Modeling birefringence characteristics and realization," *IEEE Photon. Technol. Lett.*, vol. 16, no. 5, pp. 1301–1303, May 2004.
[11] A. Ortigosa-Blance, A. Diez, M. Delgado-Pinar, J. L. Cruz, and M. V. Andres, "Ultrahigh birefringent nonlinear microstructured fiber," *IEEE Photon. Technol. Lett.*, vol. 16, no. 7, pp. 1667–1669, Jul. 2004.
[12] J. R. Simpson, R. H. Stolen, F. M. Sears, W. Pleibel, J. B. Macchesney, and R. E. Howard, "A single-polarization fiber," *J. Lightw. Technol.,* vol. LT-1, no. 2, pp. 370–373, Jun. 1983.
[13] M. J. Messerly, J. R. Onstott, and R. C. Mikkelson, "A broad-band single polarization optical fiber," *J. Lightw. Technol.*, vol. 9, no. 7, pp. 817–820, Jul. 1991.
[14] K. Okamoto, "Single-polarization operation in highly birefringent optical fibers," *Appl. Opt.*, vol. 23, no. 15, pp. 2638–2642, Aug. 1984.
[15] K. Saitoh and M. Koshiba, "Single-polarization single-mode photonic crystal fibers," *IEEE Photon. Technol. Lett.*, vol. 15, no. 10, pp. 1384–1386, Oct. 2003.
[16] H. Kubota, S. Kawanishi, S. Koyanagi, M. Tanaka, and S. Yamaguchi, "Absolutely single polarization photonic crystal fiber," *IEEE Photon. Technol. Lett.*, vol. 16, no. 1, pp. 182–184, Jan. 2004.
[17] J. Ju, W. Jin, and M. S. Demokan, "Properties of a highly birefringent photonic crystal fiber," *IEEE Photon. Technol. Lett.*, vol. 15, no. 10, pp. 1375–1377, Oct. 2001.
[18] M. Koshiba and K. Saitoh, "Finite-element analysis of birefringence and dispersion properties in actual and idealized holey-fiber structures," *Appl. Opt.*, vol. 42, no. 31, pp. 6267–6275, Nov. 2003.
[19] D. Marcuse, *Light Transmission Optics*. New York: Van Nostrand Reinhold, 1982, ch. 8 and 12.
[20] G. Kakarantzas, A. Ortigosa-Blanch, T. A. Birks, P. S. J. Russell, L. Farr, F. Couny, and B. J. Mangan, "Structural rocking filters in highly birefringent photonic crystal fiber," *Opt. Lett.*, vol. 28, no. 3, pp. 158–160, Feb. 2003.
[21] T. P. White, R. C. McPhedran, C. M. de Sterke, L. C. Botten, and M. J. Steel, "Confinement losses in microstructured optical fibers," *Opt. Lett.*, vol. 26, no. 21, pp. 1660–1662, Nov. 2001.
[22] D. Ferranrini, L. Vincetti, M. Zoboli, A. Cucinotta, and S. Selleri, "Leakage properties of photonic crystal fibers," *Opt. Express*, vol. 10, no. 7, pp. 1314–1319, Nov. 2002.
[23] N. A. Mortensen, "Effective area of photonic crystal fibers," *Opt. Express*, vol. 10, no. 7, pp. 341–348, Apr. 2002.
[24] *SMF-28e Fiber Production Information Sheet*, Corning Inc., Corning, NY, 2003.

Jian Ju was born in Hubei, China, on August 26, 1978. He received the B.Eng. degree in optoelectronics from Harbin Engineering University, Harbin, China, in 2000 and is currently working toward the Ph.D. degree at the Department of Electrical Engineering, The Hong Kong Polytechnic University, Hong Kong.

After graduation, he worked as a Teaching Assistant at the Physics Department, Harbin Engineering University, for a year and a half. His current research interests include modeling and characterization of photonic crystal fibers, photonic crystal fiber devices, and optical fiber sensors.

Wei Jin (M'95–SM'98), photograph and biography not available at the time of publication.

M. Suleyman Demokan (SM'89), photograph and biography not available at the time of publication.